The characterisation of metal-thin insulator-n-p+ silicon switching devices

J. Buxo, A.E. Owen, Gérard Sarrabayrouse, J.P. Sebaa

To cite this version:

J. Buxo, A.E. Owen, Gérard Sarrabayrouse, J.P. Sebaa. The characterisation of metal-thin insulator-n-p+ silicon switching devices. Revue de Physique Appliquée, Société française de physique / EDP, 1978, 13 (12), pp.767-770. 10.1051/rphysap:019780013012076700 . jpa-00244543

HAL Id: jpa-00244543

https://hal.archives-ouvertes.fr/jpa-00244543

Submitted on 1 Jan 1978

REVUE DE PHYSIQUE APPLIQUÉE TOME 13, DÉCEMBRE 1978, PAGE 767

VARIOUS DEVICES.

THE CHARACTERISATION OF METAL-THIN INSULATOR-n-p$^+$ SILICON SWITCHING DEVICES

J. BUXO, A. E. OWEN (*), G. SARRABAYROUSE and J. P. SEBAA

Laboratoire d'Automatique et d'Analyse des Systèmes du C.N.R.S.,
7, avenue du Colonel-Roche, 31400 Toulouse, France

Résumé. — Les auteurs présentent des résultats expérimentaux sur les caractéristiques de commutation des dispositifs MISS comportant une couche mince d'oxyde (< 50 Å) ; les résultats portent notamment sur les effets thermiques, la modulation apportée par un courant de base et enfin les effets dynamiques. L'analyse physique est conduite à l'aide d'un modèle à contre réaction dont les éléments sont décrits. Un bon accord théorie-expérience est obtenu.

Abstract. — Experiments are reported on the switching characteristics of MISS devices incorporating a thin (< 50 Å) oxide layer, including the influence of a modulating base current, the effect of temperature and the dynamic performance. A quantitative analysis of a regenerative model of switching is briefly described and shown to give a good account of the experimental results.

1. **Introduction.** — There have been several recent reports of potentially useful bistable switching properties in metal-insulator-n-p$^+$ (or -p-n$^+$) structures on silicon (i.e. MISS devices) [1-6]. It is necessary for the insulator to be either thin enough (e.g. < 50 Å) to pass substantial tunnelling currents, or for it to be otherwise *semi-insulating* [3], [5]. Switching occurs, at a critical voltage (the switching voltage V_s), when the p$^+$-n (or n$^+$-p) junction is biased in the forward direction; with the opposite polarity the characteristics are similar to those of a reverse-biased p-n junction. The switching voltage can be modulated through the influence of an additional (third) contact to the intermediate Si layer [3], [4], and Yamomoto *et al.* [4] have shown that by utilizing this feature, MISS devices could be applied to logic systems such as shift registers. Yamomoto and Morimoto [1] have also suggested that MISS devices could be light sensitive and hence used, for example, as optically-modulated switches.

For the two terminal device, Simmons and El-Badry [5] have developed two simple electrostatic models based on punch-through and avalanche mechanisms appropriate, respectively, to lightly ($< 10^{15}$ cm^{-3}) and heavily ($> 10^{17}$ cm^{-3}) doped intermediate Si layers. The equations predicted by these models are, in fact, in reasonable agreement with the results of El-Badry and Simmons [6]. However the experiments described in [1-4] have been carried out with Si of medium doping levels ($\gtrsim 10^{15}$ cm^{-3}) and neither these results, nor our own, fit the models of Simmons and El-Badry [5].

This paper presents more detailed results than hitherto on the essential characteristics of MISS switches, particularly on their temperature dependence, the influence of a modulating base current (through a third contact) and on the dynamic performance. We also describe the basic features of an alternative theory which gives good agreement with experiment and is capable of being extended to give a complete description of both the static and dynamic switching characteristics, including the ON-state and the negative resistance region.

2. **Device fabrication.** — MISS switches were fabricated from Si n-epitaxial layers (doping level $= 2 \times 10^{15}$ cm^{-3} and 7 μm thick) on p$^+$-substrates with a thin oxide layer thermally grown on the n-type Si

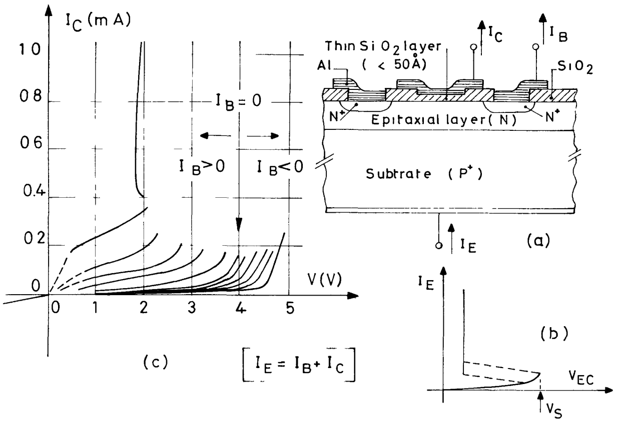

FIG. 1. — *a*) Schematic illustration of the device structure. Epitaxial layer doping density : 2×10^{15} cm^{-3}; p$^+$-substrate : 6×10^{18} cm^{-3}. Epitaxial layer thickness ~ 7 μm; substrate ~ 200 μm. Diameter of thin oxide region : 80 μm; n$^+$-annulus : 400 μm. *b*) Static switching characteristic (schematic). *c*) Experimental results for a typical device, also illustrating the effect of a base current (taken from oscilloscope traces). The curves to the right and left of $I_B = 0$ correspond to steps in I_B of 0.05 mA, with I_B positive and negative respectively.

(*) Permanent address : Department of Electrical Engineering, University of Edinburgh, King's Buildings, Edinburgh EHG 3JL, Scotland, Grande-Bretagne.

by a low temperature process (oxidation at 700 °C for 30 or 60 min in dry O_2). The structure is illustrated schematically in figure 1*a*. For modulation experiments an n^+-diffused contact was made to the n-layer; evaporated aluminium or gold contacts were made to the thin oxide and to the n^+-region, and a gold contact was made to the p^+-substrate. The diameter of the thin oxide region is 80 μm and of the n^+-annulus 400 μm.

3. **Experimental results.** — 3.1 STATIC MEASUREMENTS. — Figure 1*b* is a schematic illustration of the *I-V* curve as obtained on a typical transistor curve-tracer; similar results would be expected from a slow-ramp or a d.c. experiment. For the present purposes the p^+-substrate is called the emitter (E), the contact to the thin oxide the collector (C) and the n^+-contact to the intermediate Si layer the base (B). Figures 1*a* and *b* then define the current and voltage directions with the arrows in figure 1*a* indicating conventional current. The device switches at the voltage V_s with a positive potential V_{EC} applied between emitter and collector. Typical experimental results, taken from oscilloscope traces, are shown in figure 1*c*, which also illustrates the influence of a base current; with I_B negative V_S increases and *vice-versa*. The different traces in figure 1*c* correspond to steps of 0.05 mA in I_B for both directions from $I_B = 0$. Note that the low-impedance ON-state characteristic remains unchanged.

Measurements have also been made of the static characteristics as a function of temperature with the results, for another device, shown in figure 2. The curves labelled (1) to (7) correspond to temperatures ranging from − 193.5 to 40 °C (see figure caption for details). There is a significant change with temperature, particularly in the switching voltage V_S and this is shown explicitly for another device, in figure 3. According to the present results V_S increases as temperature decreases and seems to saturate at about − 200 °C; so far, however, experiments have not been taken to lower temperature to determine whether V_S remains constant or goes through a maximum. These appreciable effects of temperature are in marked contrast to the results of El-Badry and Simmons [6]; they found essentially no change in V_S, although they did observe a small effect on the ON-state characteristic but in the opposite sense to that shown in figure 2.

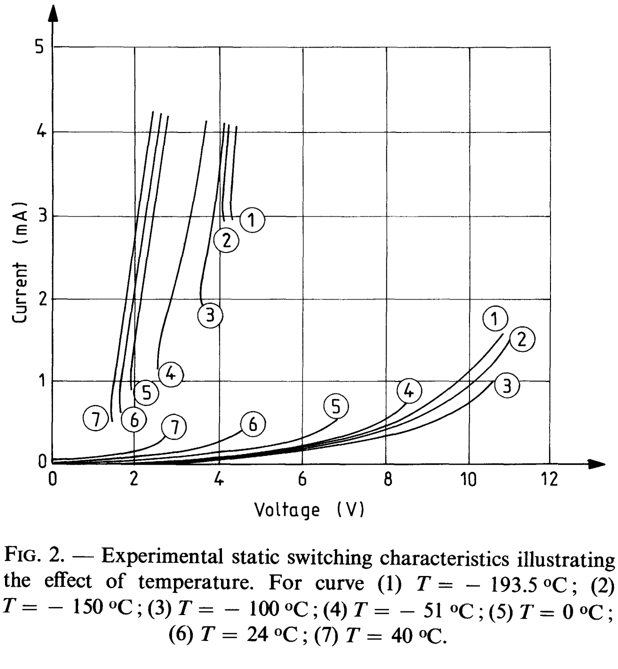

FIG. 2. — Experimental static switching characteristics illustrating the effect of temperature. For curve (1) $T = -193.5$ °C; (2) $T = -150$ °C; (3) $T = -100$ °C; (4) $T = -51$ °C; (5) $T = 0$ °C; (6) $T = 24$ °C; (7) $T = 40$ °C.

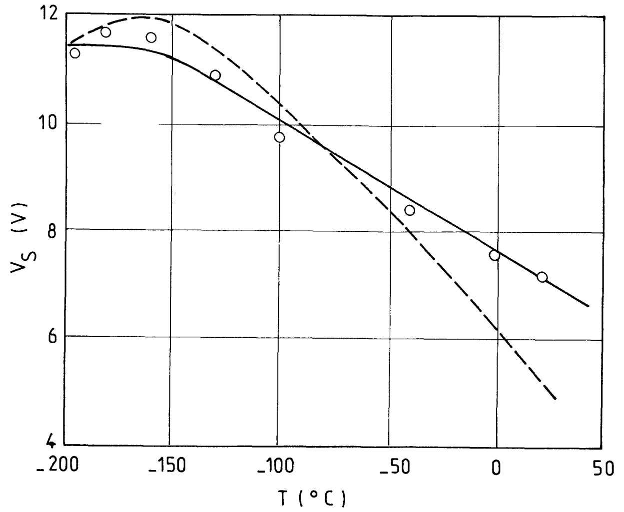

FIG. 3. — The variation of switching voltage V_S with temperature for a typical device. The dashed curve was calculated from equation (2) with the following values of the variables: $(\varphi_M - \chi) = 0.03$ eV; $\delta = 20$ Å : $\gamma = 7.45$ (dimensionless) : $N_D = 2 \times 10^{15}$ cm^{-3}; $J_\sigma = 1.3 \times 10^4$ A.cm^{-2} corresponding to a surface state density $N_{SS}^A = 8 \times 10^{12}$ cm^{-2} eV^{-1}; $\sigma_n = 10^{-16}$ cm^2; $v_{th} = 10^7$ cm.s^{-1}.

3.2 DYNAMIC MEASUREMENTS. — When a voltage pulse of magnitude greater than V_S is applied to an MISS switch, the current through the device remains low (essentially the OFF-state current) for a period t_D, after which it rises more or less instantaneously to the ON-state current, i.e. there is a delay time (t_D) before switching takes place. Figure 4 illustrates this for three pulses of different magnitude; as the applied pulse height increases (with respect to V_S) the delay time decreases. The shape of the current response appears to be controled by the internal switching mechanisms of the device and is independent from the external circuit used for the measurements. In figure 4 the current seems to rise from its OFF to ON-state values in a *two-stage* process; this was a common but not universal feature of our measurements : for the range of pulse heights used, t_D is of the order 10^{-8}-10^{-5} seconds. Kroger and Wegener [2] report delay times as short as a few nanoseconds or less, but they applied pulses rather greater in magnitude than those used for the present studies.

The base current also influences the delay time and figure 5 illustrates the combined effects of I_B and pulse height on t_D. In figure 5*b* t_D is plotted as a function of

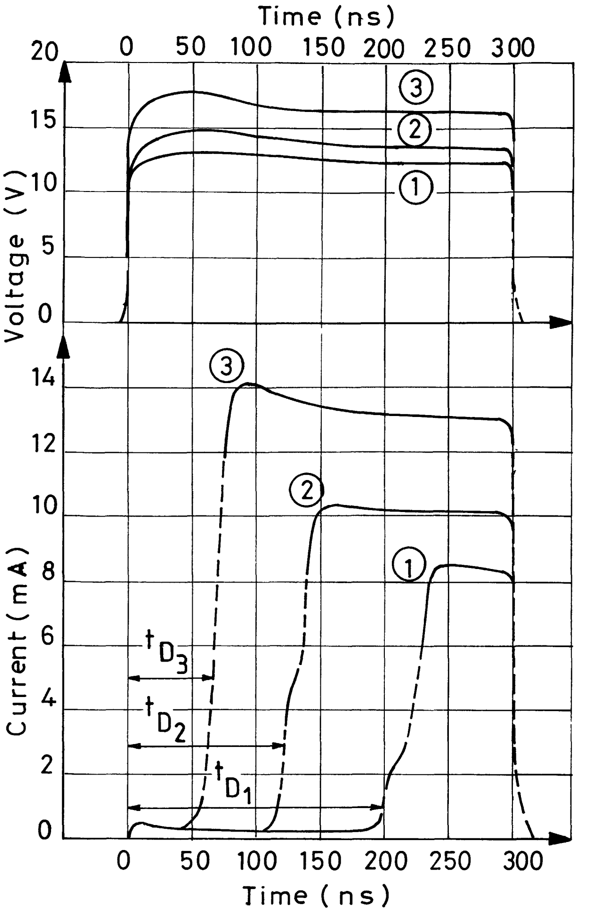

FIG. 4. — Illustrating the influence of voltage pulse height on the switching delay time t_D. Curves (1), (2) and (3) correspond to pulses of increasing voltage.

I_B (positive and negative) with pulse height as a parameter. For completeness figure 5*a* shows the variation of switching voltage V_S as a function of base current; I_B can be regarded as influencing t_D through its effect on V_S.

4. **Discussion.** — It seems clear that the punch-through and avalanche models of MISS switching, developped by Simmons and El-Dadry [5], do not apply to our own results nor, most likely, to the results of other workers [1-4]. Yamamoto and Morimoto [1] have already tentatively suggested the possibility of a regenerative mechanism of switching related to the build-up of an inverted region in the Si at the Si-SiO$_2$ interface. In the following we give a brief description of the quantitative development of such a model. The essential features of the model are given in figure 6 which shows the band structure of the OFF- and ON-states; it also defines the parameters used in the following discussion. It is necessary to solve the continuity equations for both the majority J_n and minority carrier current J_p, taking into account the link between J_n and J_p imposed by the presence of the p$^+$ n junction. The numerical solution of these equations has been carried out and a continuous description of the static *I-V* characteristic is obtained, including the negative resistance region. Preliminary calculations also show that the regenerative model is capable of describing pulsed operation (dynamic performance) but for reasons of space the present discussion is restricted to considering the switching voltage V_S and the ON-state characteristic.

Throughout the OFF-state characteristic the voltage V_{EC} is practically confined to the MIS part of the structure. The continuity equation for the transport

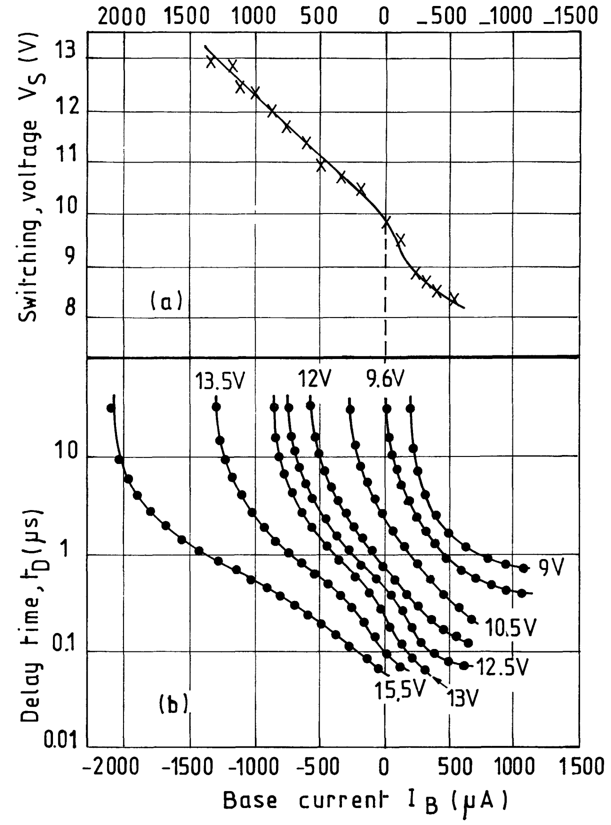

FIG. 5. — *a*) The switching voltage V_S as a function of base current I_B. *b*) The delay time t_D as a function of I_B for different voltage pulse heights.

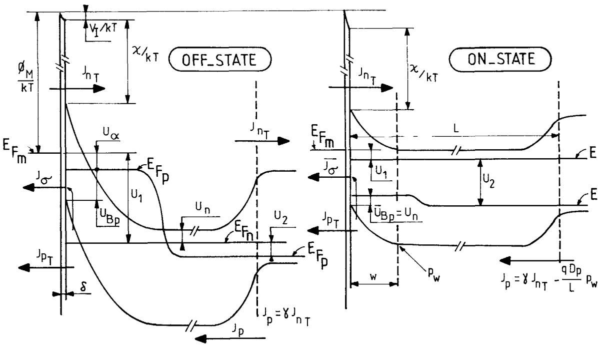

FIG. 6. — Schematic illustration of the energy-band structures of the OFF- and ON-states for the regenerative model of switching. The diagram also defines some of the parameters introduced in the text.

of minority carriers has been discussed previously [7], [8], and for the present case it is written as follows :

$$J_p = \gamma A^* \alpha_n T^2 \exp\left[-\frac{(\varphi_M - \chi - V_I)}{kT}\right] \times \\ \times [1 - \exp(-U_1)] \\ = A^* \alpha_p T^2 \exp(-U_{B_p}) [1 - \exp(-U_\alpha)] + J_\sigma \qquad (1)$$

where γ is the p$^+$ n junction efficiency [9], J_σ the fraction of the diffusion current that tunnels *via* the acceptor state density [10], α_n and α_p are tunnelling attenuation factors [7], A^* is the Richardson constant, T the temperature and k the Boltzmann constant. The other parameters are as defined in figure 6. Equation (1), together with the expression which relates the voltage across the oxide layer, V_I, to the applied voltage ($\approx V_1 = (kT/q)\, U_1$) [8], gives a description of the OFF-state characteristic. As soon as the inversion situation occurs i.e. : $U_{B_p} = \bar{U}_{B_p} = U_n$ (where $\bar{U}_{B_p}$ is the saturation value of U_{B_p} at inversion), the majority carrier driving current of the regenerative system, J_{nT}, will tend to increase rapidly because the inversion layer imposes larger field values across the oxide, thereby making $[(\varphi_M - \chi - V_I)/kT]$ decrease. The minority carrier current given by equation (1) will then have to adapt to the condition $U_{B_p} = \bar{U}_{B_p}$, which remains unchanged once the inversion situation is reached. As a result, the control of J_{nT} is obtained with much lower values of U_1 in order to satisfy equation (1), i.e. the system switches to the ON-state. By setting U_{B_p} equal to U_n in equation (1) we can derive the voltage $V_S \approx U_1(kT/q)$ at which the inversion situation is first established, i.e. the switching voltage. We obtain :

$$V_S = \frac{\varepsilon_I^2\, \varepsilon_0}{2\, qN_D\, \varepsilon_S\, \delta^2} \times \\ \times \left[\varphi_M - \chi - kT \ln \left\{ \frac{\gamma \sqrt{N_c N_v}}{N_D[1 + (\bar{J}_\sigma / A^* T^2 \alpha_n)]} \right\}\right]^2 \\ + kT \ln \left(\frac{\sqrt{N_c N_v}}{N_D} \right) - (\varphi_M - \chi) \qquad (2)$$

where N_v and N_c are the densities of state in the valence and conduction bands respectively, N_D is the doping level, and ε_I, ε_S, ε_0 are the insulator, silicon and vacuum permittivities.

$$\bar{J}_\sigma = qN_{SS}^A\, \sigma_p\, v_{th}\, N_v[E_g - (\varphi_M - \chi)]$$

where N_{SS}^A is the acceptor state density, σ_p the acceptor state capture cross section and v_{th} the thermal velocity [10]. With reasonable values of the parameters involved, equation (2) gives a good approximation to the magnitude of V_S and its temperature dependence as can be seen from figure 3. The dashed line in figure 3 was calculated from equation (2), with the variables set at the values given in the caption. It is possible to obtain an even better fit between theory and experiment by including, for example, the variation in the width of the space-charge region in the Si at the Si-SiO$_2$ interface, but the more cumbersome computation process involved has not yet been completed. For the present purposes it is sufficient to note that the model leading to equation (2) provides an adequate description of the experimental data on V_S. It could also be extended to include the influence of base current I_B on V_S.

The ON-state can be analysed but a new boundary condition for the diffusing minority carriers must be introduced because of the collapse of the barrier at the oxide-semiconductor interface. The appropriate equation is :

$$\gamma A^* \alpha_n T^2 \exp\left[-\frac{(\varphi_M - \chi - V_I)}{kT}\right] \times \\ \times [1 - \exp(-U_1)] - \left(\frac{qD_p}{L}\right) p_W = \\ = A^* \alpha_p T^2 \exp(-\bar{U}_{p_p}) + \bar{J}_\sigma \qquad (3)$$

where D_p is the diffusion coefficient of the minority carriers, L the width of the intermediate (n) Si layer and p_W the minority carrier density at the edge of the MIS space-charge region.

A more complete account of the regenerative model, including its application to the effect of a base current, the negative resistance region and dynamic operation, will be published elsewhere. Clearly however, it is capable of providing a good approximation to our results and, possibly, to those of other workers. Since the models of Simmons and El-Badry also fit reasonably well to their particular results [5], [6], one must conclude, for the time being, that there are at least three operating mechanisms of MISS switches : punch-through, regeneration and avalanche mechanisms. Which one is dominant presumably depends on device parameters such as the doping level and width of the intermediate Si layer.

References

[1] Yamomoto T. and Morimoto, H., *Appl. Phys. Lett.* **20** (1972) 269.

[2] Kroger, H. and Wegener, H. A. R., *ibid.* **23** (1973) 397.

[3] Kroger, H. and Wegener, H. A. R., *ibid.* **27** (1975) 303.

[4] Yamomoto, T., Kawamura, K. and Shimizu, H., *Solid State Electron.* **19** (1976) 701.

[5] Simmons, J. G. and El-Badry, A., *ibid.* **20** (1977) 955.

[6] El-Badry, A. and Simmons, J. G., *ibid.* **20** (1977) 963.

[7] Buxo, J., Estève, D. and Sarrabayrouse, G., *Phys. Status Solidi* (*a*) **37** (1976) K 105.

[8] Buxo, J., Sarrabayrouse, G. and Estève, D., *ibid.* **42** (1977) 173.

[9] Lindmayer, J. and Wrigley, C. Y., *Semiconductor Devices* (Van Nootrand Princeton) 1965.

[10] Sarrabayrouse, G., Buxo, J. and Estève, D., *Phys. Status Solidi* **46** (1978) 185.